A finite element based approach to observe hydrodynamic pressure in reservoir adjacent to concrete gravity dam

Santosh Kumar Das[*], Kalyan Kumar Mandal and Arup Guha Niyogi

Department of Civil Engineering, Jadavpur University, Kolkata-32, India

Abstract. This paper deals with the study of hydrodynamic pressure in reservoir adjacent to the concrete gravity dam subjected to dynamic excitation. Widely famous finite element method is used to discretize the reservoir domain for modelling purpose. Pressure is considered as nodal variable following Eulerian approach. A suitable nonreflecting boundary condition is applied at truncated face of reservoir to make the infinite reservoir to finite one for saving the computational cost. Thorough studies have been done on generation of hydrodynamic pressure in reservoir with variation of different geometrical properties. Velocity profile and hydrodynamic pressure are observed due to harmonic excitation for variation of inclination angle of dam reservoir interface. Effect of bottom slope angle and inclined length of reservoir bottom on hydrodynamic pressure coefficient of reservoir are also observed. There is significant increase in hydrodynamic pressure and distinct changes in velocity profile of reservoir are noticeable for change in inclination angle of dam reservoir interface. Change of bottom slope and inclined length of reservoir bottom are also governing factor for variation of hydrodynamic pressure in reservoir subjected to dynamic excitation.

Keywords: earthquake excitation; Eulerian approach; finite element; hydrodynamic pressure; infinite reservoir

1. Introduction

Stability of gravity dam highly influenced by the behavior of adjacent reservoir. Hydrodynamic pressure developed on dam reservoir interface due to earthquake excitation. Various authors have studied the effect of hydrodynamic pressure on dam due to presence of adjacent reservoir under dynamic excitation. First Westergaard (1933) developed the formulation for hydrodynamic pressure distribution on the face of dam subjected to earthquake. Saini *et al*. (1978) used finite element method for analysis of dam reservoir coupled system due to horizontal ground acceleration. Hall and Chopra (1982) performed the analysis of concrete gravity dam along with the hydrodynamic effect. Humar and Roufaiel (1983) used finite element method for calculation of hydrodynamic pressure in reservoir adjacent to a gravity dam subjected to harmonic ground motion. Sharan (1985) studied the hydrodynamic pressure due to vibration of a structure within unbounded fluid medium using finite element technic. Sharan (1987) proposed a technic for modeling the radiation damping for analysis of hydrodynamic pressure due to vibration of a structure submerged in compressible

---

∗Corresponding author, Assistant Professor, E-mail: santoshatju@gmail.com

fluid. Tsai *et al.* (1990) applied a semi analytical technic to study the dam reservoir interaction within time domain. Li *et al.* (1996) performed the analysis of dam reservoir system with an efficient boundary condition utilizing finite element technique. Calayir *et al.* (1996) performed the earthquake analysis of dam reservoir coupled system using both Eulerian and Lagrangian approach. Maity and Bhattacharyya (1999) analyzed a reservoir using finite element method with a special far boundary condition within time domain. Bouaanani *et al.* (2003) developed a closed form formulation for determination of hydrodynamic pressure on gravity dam subjected to earthquake. Kucukarslan *et al.* (2005) investigated dam reservoir interaction considering reservoir bottom absorption effects. Gogoi and Maity (2006) presented a non-reflecting boundary condition for modelling of infinite reservoir using finite element technic. Samii and Lotfi (2007) used modal approaches for analytical study of concrete gravity dam subjected to earthquake excitation. Wang *et* al. (2011) used finite element method in time domain to analyze offshore structures. Wang *et al.* (2011) developed a doubly asymptotic open boundary condition for study of dam reservoir system within time domain. Attarnejada and Bagheri (2011) studied the effect of vertical and horizontal component of earthquake for transient analysis of dam-reservoir system in time domain. Neya and Ardeshir (2013) proposed a solution for determination of hydrodynamic pressure considering viscosity of fluid and wave absorption of reservoir. Pelecanos *et al.* (2016) studied the dam reservoir interaction effect on response of concrete and earthen dams subjected to dynamic load. Adhikary and Mandal (2018) used eight node isoparametric element to discretize the fluid medium and solved the problem using pressure based formulation. Humaish *et al.* (2018) performed an experimental work to study the response of gravity dam subjected to earthquake excitation. Eftekhari and Jafari (2018) proposed a formulation using Ritz method for dynamic analysis of dam-reservoir system. Wang *et al.* (2018) proposed a correction for westergaard formula to study the hydrodynamic pressure on the face of gravity dam with varying height. Sharma *et al.* (2019) presented a space-time finite element method for study of dam-reservoir-soil interaction subjected to earthquake excitation. Gao Yichao *et al* (2019) developed a procedure for dynamic analysis of dam-reservoir system with a new higher order doubly asymptotic open boundary. Barzegar and Palaniappan (2020) used both fully reflective boundary and absorbing boundary condition for analyzing the structure submerged in fluid. Khaivi and Sari (2021) investigated the hydrodynamic pressure in reservoir adjacent to concrete gravity dam subjected to vertical component of vibration with the help of an analytical solution. Nguyen *et al.* (2021) studied the velocity profile and variation of pressure inside the fluid medium using Smoothed Particle Hydrodynamics model.

For design of gravity dam study on hydrodynamic pressure due to the adjacent reservoir is very much important. Geometry of the adjacent reservoir is an important parameter for this purpose. Very limited works has been reported on study of hydrodynamic pressure of infinite reservoir with inclined bottom surface. Most of the previous researchers have modeled the fluid domain using finite element method with different field variables such as displacement, velocity potential, pressure etc. Out of which displacement based formulation leads to the presence of spurious or circulation modes, i.e., non-irrotational modes which have no physical meaning. These circulation modes may correspond to zero frequencies. In the present study pressure has been considered as unknown variable in the liquid domain. Present work has been done on infinite reservoir having inclined dam reservoir interface and also with inclined bottom surface following Eulerian approach. In this method nodal variable reduced to a single valued unknown variable so that it can be easy to handle for computation purpose. In this study, dam is considered to be as rigid and the bottom of the reservoir is assumed as absorptive. Effect of surface wave have been neglected throughout the study.

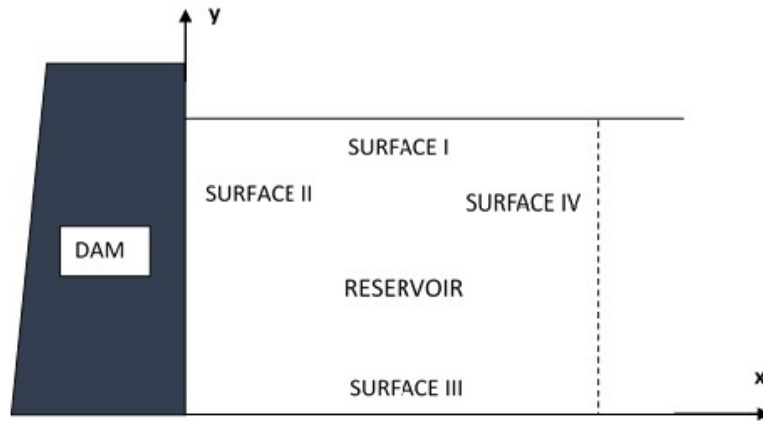The infinite reservoir is truncated at a suitable distance to save the computational time. An

Fig. 1 schematic diagram of dam and reservoir system

appropriate nonreflecting boundary condition is applied at the truncated face of the reservoir. Fluid is assumed as compressible and inviscid. The domain of reservoir discretized by eight node finite element. Variation of hydrodynamic pressure with inclined dam reservoir interface has been determined for dynamic excitation. Nature of hydrodynamic pressure due to change in bottom slope of the reservoir has been thoroughly observed. Effect of inclined length of reservoir bottom on the hydrodynamic pressure is also studied. A MATLAB code has been developed for the current study and Newmark's time integration method is adopted to solve the dynamic equilibrium equation.

2. Theoretical formulation

The analysis is carried out assuming two dimensional system. The medium of reservoir fluid is assumed as compressible and inviscid. Hydrodynamic pressure generated due to external excitation is given as below.

$$\nabla^2 p(x, y, t) = \frac{1}{C^2}\ddot{p}\ (x, y, t) \tag{1}$$

Here C is the velocity of the wave in fluid and ∇^2 is the Laplace operator in two dimension in the fluid medium. The hydrodynamic pressure distribution can be computed by solving Eq. (1). The geometry of the dam-reservoir system is shown in Fig. 1.

At the free surface (surface I), considering the effect of surface wave of fluid, the boundary condition can be taken as follows.

$$\frac{1}{g}\ddot{p} + \frac{\partial p}{\partial y} = 0 \tag{2}$$

However, neglecting the effects of surface wave of water, the boundary condition of the free surface of reservoir may be taken as below.

$$p\big(x, H_f\ \big) = 0 \tag{3}$$

Here, H_f is the depth of the reservoir.

At dam-reservoir interface (surface II), the pressure has to satisfy following condition.

$$\frac{\partial p}{\partial n}(0, y, t) = \rho_f a e^{i\omega t} \tag{4}$$

Here $ae^{i\omega t}$ is the horizontal component of the ground motion in which, ω is the circular frequency of vibration and $i=\sqrt{-1}$, n is the outwardly directed normal between interface of dam and reservoir. ρ_f is the density of fluid.

At bottom surface (surface III) of the reservoir, considering the absorption of pressure wave, pressure should satisfy the following equation.

$$\frac{p}{\partial n}(x, 0, t) = i\omega q\dot{p} \ (x, 0, t) \tag{5}$$

Here

$$q = \frac{1}{C}\left(\frac{1-\alpha}{1+\alpha}\right) \tag{6}$$

α is the reflection coefficient.

At the truncation surface of reservoir (surface IV), the implementation of boundary condition is an important feature for analysis of infinite fluid medium. The boundary condition at the truncated surface may be written as follows.

$$\frac{\partial p}{\partial n} = \left(\xi_m - \frac{1}{C}\right)\dot{p} \tag{7}$$

According to Gogoi and Maity (2006) ξ_m is obtained as follows.

$$\zeta_m = -\frac{i\sum_{m=1}^{\infty}\frac{\lambda_m{}^2 I_m}{\beta_m}e^{(-k_m x)}(\Psi_m)}{\Omega C \sum_{m=1}^{\infty}\frac{\lambda_m{}^2 I_m}{\beta_m k_m}e^{(-k_m x)}(\Psi_m)} \tag{8}$$

If the effect of surface wave is neglected, then χ can be considered to be zero.

Using the Galarkin technique and considering pressure to be the nodal unknown variable, the Eq. (1) can be discretized as below.

$$\int_\Omega N_{rj}\left[\nabla^2 \sum N_{ri}p_i - \frac{1}{c^2}\sum N_{ri}\ddot{p}_\iota\right]d\Omega = 0 \tag{9}$$

Where N_{ij} is the interpolation function for the reservoir and Ω is the region of interest. Now using Green's theorem Eq. (9) may be transformed to the following equation.

$$-\int_\Omega \left[\frac{\partial N_{rj}}{\partial x}\sum\frac{\partial N_{ri}}{\partial x}p_i + \frac{\partial N_{rj}}{\partial y}\sum\frac{\partial N_{ri}}{\partial y}p_i\right]d\Omega - \frac{1}{c^2}\int_\Omega N_{rj}\sum N_{ri}\,d\Omega\ddot{p}_\iota + \int_\Gamma N_{rj}\sum\frac{\partial N_{rj}}{\partial n}d\Gamma p_i = 0 \tag{10}$$

Γ is the boundaries of fluid domain. The whole system of equation may be written in a matrix form as follows.

$$[\bar{J}]\{\ddot{p}\} + [\bar{H}]\{p\} = \{F\} \tag{11}$$

Where

$$[\bar{J}] = \frac{1}{c^2}\sum\int_\Omega [N_r]^T [N_r]d\Omega \tag{12}$$

$$[\bar{H}] = \sum \int_{\Omega} \left[\frac{\partial}{\partial x}[N_r]^T \frac{\partial}{\partial x}[N_r] + \frac{\partial}{\partial y}[N_r]^T \frac{\partial}{\partial y}[N_r] \right] \; d\Omega \tag{13}$$

$$\{F\} = \sum \int_{\Gamma} [N_r]^T \frac{\partial p}{\partial n} d\Gamma = \{F_f\} + \{F_{fs}\} + \{F_{fb}\} + \{F_t\} \tag{14}$$

Here the subscript *f, fs, fb* and *t* presents the free surface, fluid-structure interface, fluid-bed interface and truncation surface respectively. For free surface, $\{F_f\}$ may be written in finite element form as given below.

$$\{F_f\} = -\frac{1}{g}[R_f]\{\ddot{p}\} \tag{15}$$

$$[R_f] = \sum \int_{\Gamma_f} [N_r]^T [N_r] d\Gamma \tag{16}$$

At the fluid-structure interface, if $\{a\}$ is the vector of nodal accelerations, $\{F_{fs}\}$ may be expressed as given below.

$$\{F_{fs}\} = -\rho_f [R_{fs}]\{a\} \tag{17}$$

$$[R_{fs}] = \sum \int_{\Gamma_{fs}} [N_r]^T [T] \; [N_a] d\Gamma \tag{18}$$

Here $[T]$ is the transformation matrix at dam-reservoir interface and N_d is the interpolation function of dam.

At the reservoir bed interface $\{F_{fb}\}$ may be expressed as given below.

$$\{F_{fb}\} = i\omega q [R_{fb}]\{p\} \tag{19}$$

$$[R_{fb}] = \sum \int_{\Gamma_{fb}} [N_r]^T \; [N_r] d\Gamma \tag{20}$$

At the truncated surface $\{F_t\}$ may be expressed as given below.

$$\{F_t\} = \zeta_m [R_t]\{p\} - \frac{1}{c}[R_t]\{\dot{p}\} \tag{21}$$

$$[R_t] = \sum \int_{\Gamma_t} [N_r]^T \; [N_r] d\Gamma \tag{22}$$

After putting all the term, the Eq. (11) becomes as follows.

$$[J]\{\ddot{p}\} + [A]\dot{p} + [H]\{p\} = \{F_r\} \tag{23}$$

Where

$$[J] = [\bar{J}] + \frac{1}{g}[R_f] \tag{24}$$

$$[A] = \frac{1}{c}[R_t] \tag{25}$$

$$[H] = [\bar{H}] + \zeta_m [R_t] - i\omega q [R_{fb}] \tag{26}$$

$$\{F_r\} = -\rho_f [R_{fs}]\{a\} \tag{27}$$

Table 1 Comparison of natural frequencies of first five mode of the reservoir

Mode Number	Natural frequency (Hz)present study	Natural frequency (Hz) Samii and Lotfi
1	3.188	3.115
2	4.881	4.749
3	7.924	7.796
4	9.330	9.300
5	10.036	9.958

To solve the Eq. (23), Newmark's integration method is adopted. It has been seen that two parameters β and δ in Newmark's method may be varied to get the accuracy. In the present study, the values of δ and β used are 0.5 and 0.25, respectively. The velocity has been determined using Gild's integration technic.

3. Results and discussion

3.1 Validation of proposed algorithm

For validation of the proposed algorithm free vibration results are compared with the results of Samii and Lotfi (2007) considering width of the reservoir as 200 m and height of the reservoir as 116.19 m adjacent to the gravity dam. Velocity of wave through water is assumed as 1440 m/sec. and unit weight of water is assumed as 9.81 kN/m^3. The natural frequencies which are compared with the result given by the Samii and Lotfi (2007) are presented in Table 1.

3.2 Numerical results

3.2.1 Section I

In this paper behavior of infinite reservoir adjacent to the gravity dam has been studied. The structure is considered as rigid and the absorption effect of bottom of the reservoir is taken. The dam is subjected to earthquake excitation in the horizontal direction. Length of the reservoir is truncated at a suitable distance and the boundary condition proposed by Gogoi and Maity (2006) is applied along the truncated face to get the effect of infinite reservoir. Effect of surface wave is neglected. The reservoir domain is discretized using eight node isoparametric element. For the solution of dynamic equilibrium equation using Newmark's integration technique the time step is considered as *T/32*.

In the first section of this study, analysis is carried for harmonic excitation with the inclined dam reservoir interface (Fig. 2). Height of the reservoir (H_f) is taken as 100 m and density (ρ) of water is assumed as 1000 kg/m^3 and velocity of wave (C) in water is assumed as 1440 m/s. Length by height ratio (L/H_f) is taken as 0.1 and coefficient of reservoir bottom absorption is assumed as 0.95. Study has been done for *Tc/H$_f$ $\geq$ 4* with different angle of inclination (θ) of fluid structure interface i.e. 30°, 45°, 60° and 75°. Amplitude of sinusoidal excitation is assumed as equal to the gravitational acceleration *g*.The time history plot of hydrodynamic pressure co-efficient ($C_p = P/\rho a H_f$) at the base of the dam is shown in Figs. 3-6 for *Tc/H$_f$* = 4, 10, 50 and 100 accordingly. It is clear that
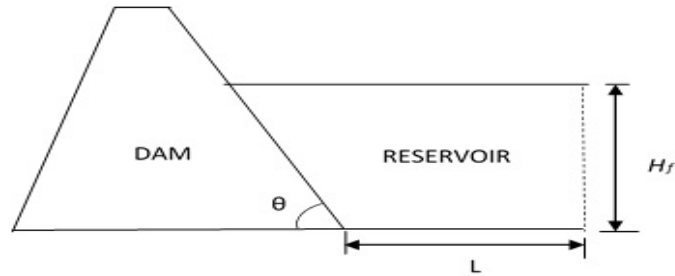
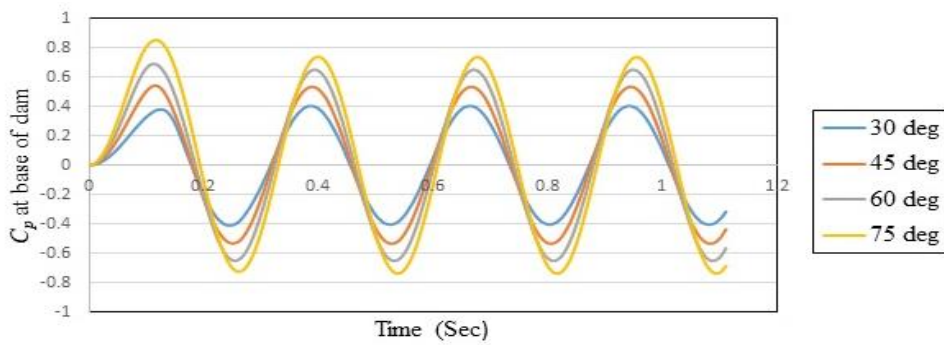Fig. 2 Geometry with inclined dam reservoir interface

Fig. 3 Time history of pressure coefficient (C_p) at base of dam at $Tc/H_f = 4$
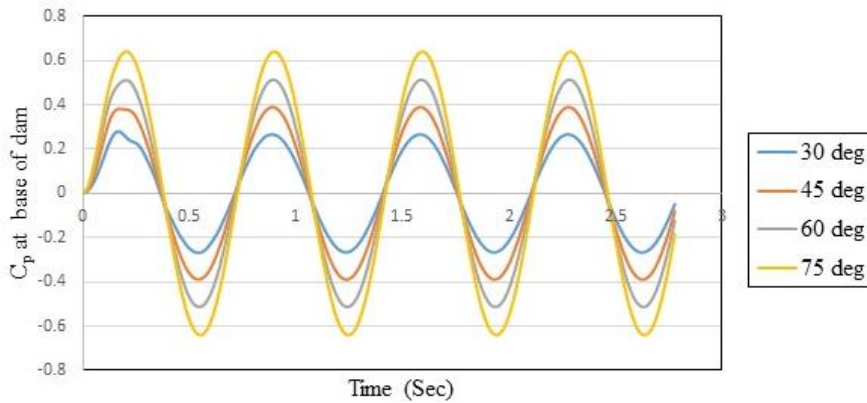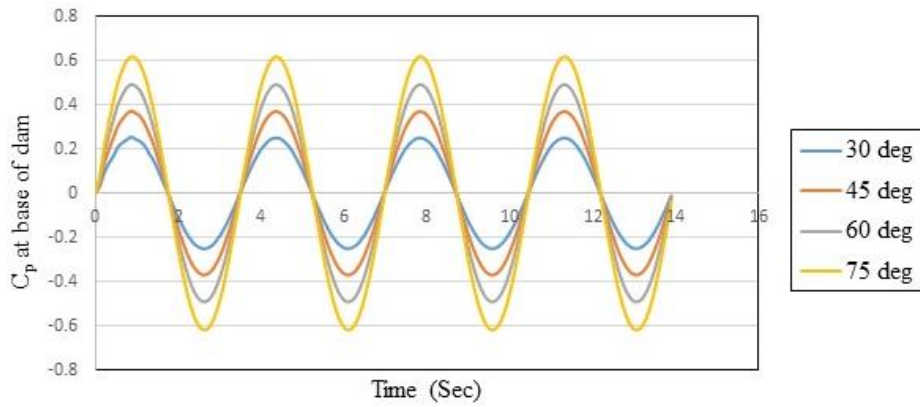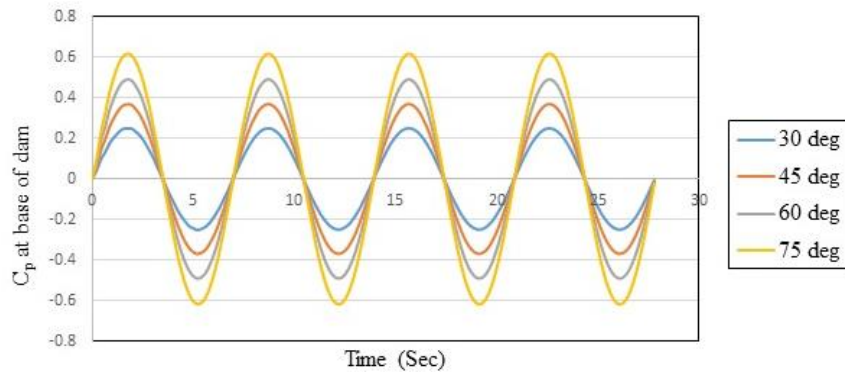

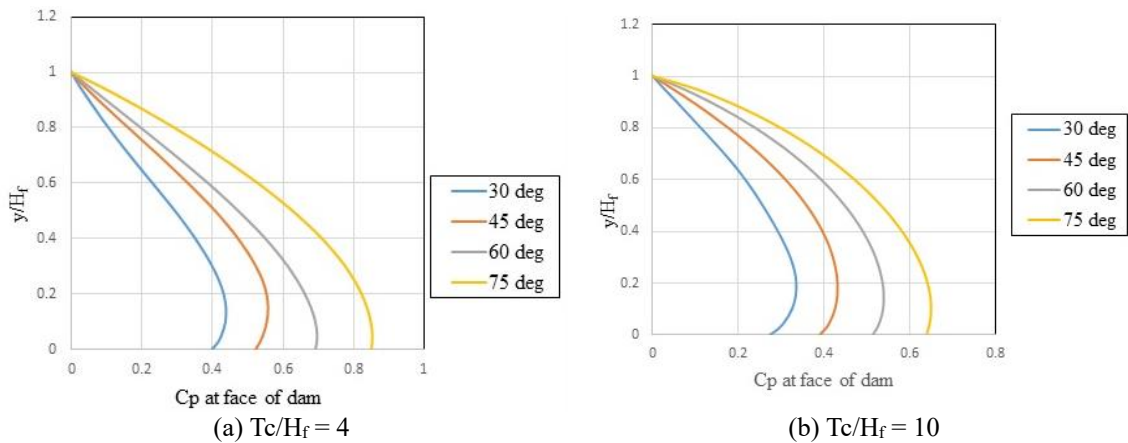Fig. 4 Time history of pressure coefficient (C_p) at base of dam at $Tc/H_f = 10$

hydrodynamic pressure increases with increase of inclination of fluid structure interface. For Tc/H_f =4 the time history curves of pressure co-efficient are leading in time axis for increase of inclination angles. But time history curves of pressure co-efficient are in the same phase of time for Tc/H_f =10, 50 and 100. Distribution of hydrodynamic pressure coefficient along the face of dam is presented in Figs. 7-8 for Tc/H_f = 4, 10, 50 and 100. From these figure it has been seen that the distribution of pressure is not uniform for $Tc/H_f = 4$. But the hydrodynamic pressure distribution is perfectly parabolic and increases with increase of inclination (θ) of dam reservoir interface for other values frequencies (Tc/H_f =10, 50 and 100). Maximum pressure occurred for $\theta = 75^o$.

Fig. 5 Time history of pressure coefficient (Cp) at base of dam at Tc/Hf = 50

Fig. 6 Time history of pressure coefficient (C_p) at base of dam at Tc/Hf = 100

(a) Tc/H$_f$ = 4   (b) Tc/H$_f$ = 10

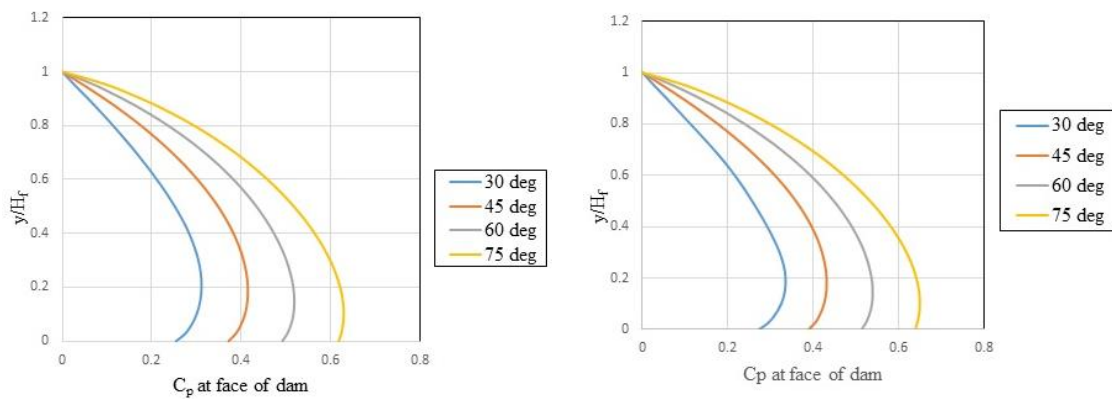Fig. 7 Distribution of pressure coefficient (Cp) at inclined face of dam

3.2.2 Section II

In this section of work velocity profile of reservoir with the variation of angle of inclination (θ) of dam reservoir interface have been studied. For this purpose, the height of the reservoir (H_f),

density of water (ρ), velocity of wave (C) in water is taken as taken in the Section I. The coefficient of reservoir bottom absorption is taken as 0.5. The study has been done with Tc/H_f =100 for values of L/H_f as 0.1 and 0.5 for sinusoidal excitation. Figs. 9-10 shows the velocity plot of fluid for coefficient of bottom absorption as 0.5, L/H_f = 0.1 and inclination (θ) of dam reservoir interface varies as 30^0, 45^0, 60^0, 75^0. Figs. 11 and 12 shows the velocity plot of fluid for coefficient of bottom absorption as 0.5, L/H_f = 0.5 and inclination (θ) of dam reservoir interface varies as 30^0, 45^0, 60^0, 75^0. From velocity plots of reservoir clear differences are noticeable for change in inclination (θ) of dam reservoir interface for both L/H_f as 0.1 and 0.5.

3.2.3 Section III

In this section of work variation of hydrodynamic pressure with the variation of inclination (θ_b) of bottom of reservoir has been studied (Fig. 13). If the bottom slope angle (θ_b) is anticlockwise then it is assumed as positive and if it is clockwise then assumed as negative. The height of the reservoir (H_f), density of water (ρ), velocity of wave (C) in water is taken as in the Section I.

(a) Tc/H_f = 50   (b) Tc/H_f = 100
Fig. 8 Distribution of pressure coefficient (Cp) at inclined face of dam

(a) θ=30^0 (b) θ=45^0
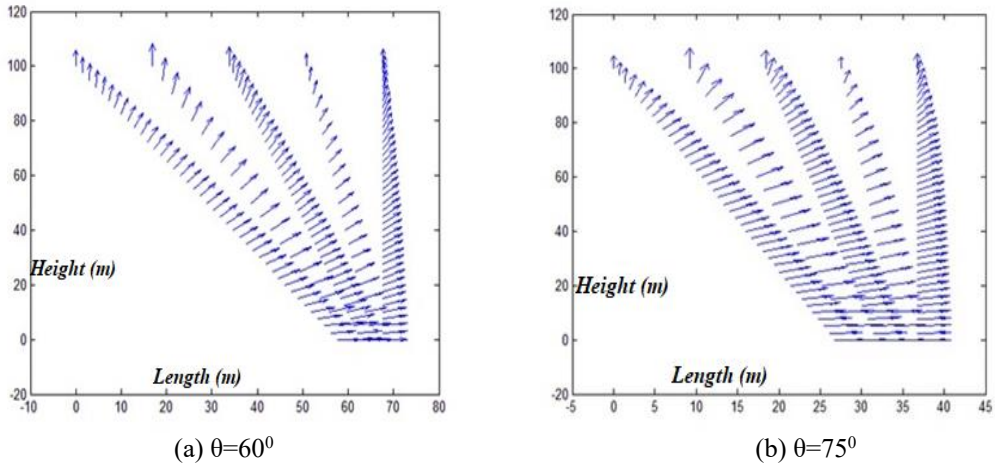Fig. 9 Velocity plot at 8.89 sec for absorption coefficient=0.5 and L/H_f = 0.1

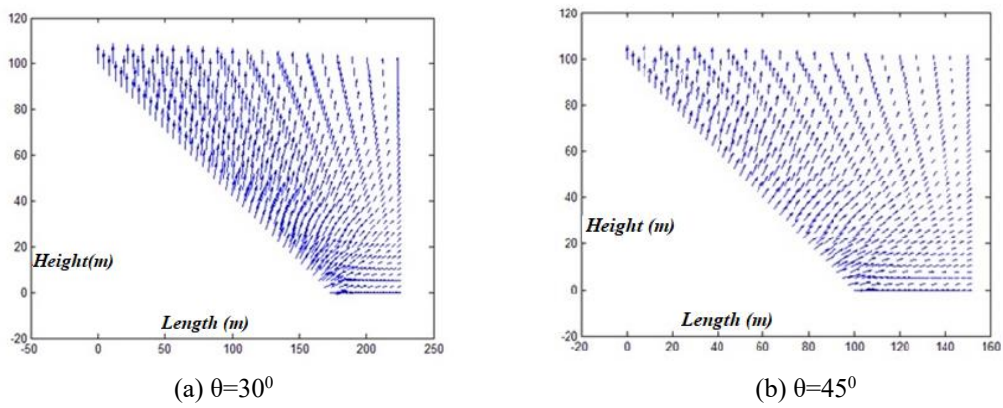(a) θ=60⁰   (b) θ=75⁰

Fig. 10 Velocity plot at 8.89 sec for absorption coefficient=0.5 and L/H_f = 0.1

(a) θ=30⁰   (b) θ=45⁰

Fig. 11 Velocity plot at 8.89 sec for absorption coefficient=0.5 and L/H_f = 0.5
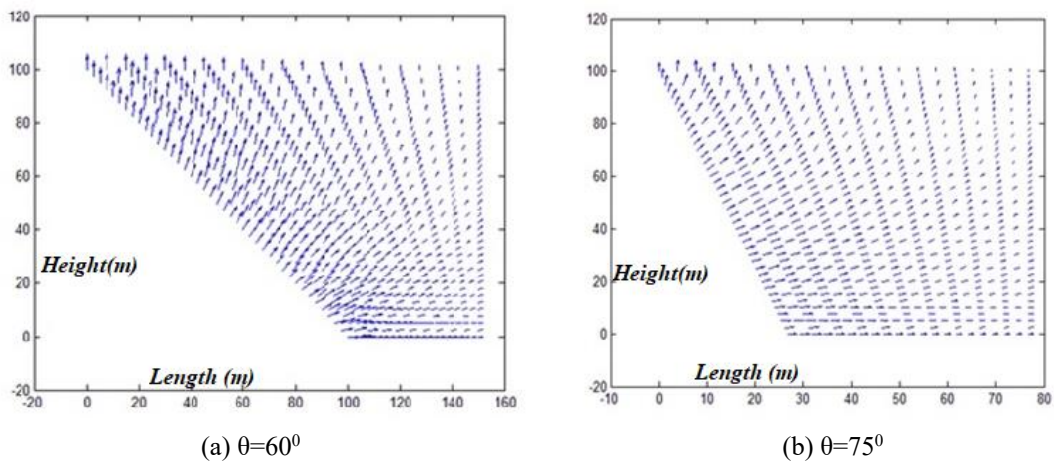

(a) θ=60⁰   (b) θ=75⁰

Fig. 12 Velocity plot at 8.89 sec for absorption coefficient=0.5 and L/H_f = 0.5

Upstream face of dam is assumed as vertical with Tc/H_f =100, L/H_f= 0.5 and coefficient of bottom absorption as 0.95. The variation of hydrodynamic pressure coefficient (C_p) with change in slope (θ_b) of reservoir bottom has been studied for sinusoidal load and also for earthquake excitation (Koyna Earthquake 1967). Fig. 14(a) shows distribution of pressure coefficient (C_p) at face of dam with different values of positive bottom slope (θ_b). This figure clearly established that the value of pressure at base of dam increases with increase of positive value of bottom slope (θ_b). Fig. 14(b) shows distribution of pressure coefficient (C_p) at face of dam with different values negative bottom slope (θ_b). This figure shows that the value of pressure at base of dam decreases with increase of negative value of bottom slope (θ_b). Figs. 15(a) and 16(a) present the time history plot of pressure coefficient (C_p) at base of dam due to Koyna Earthquake with different bottom slope (θ_b) angle for positive and negative slope accordingly. Figs. 15(b) and 16(b) present the distribution of pressure coefficient (C_p) at face of dam with different positive and negative bottom slope (θ_b) accordingly due to Koyna earthquake. It is clear from Figs. 15(b) and 16(b) that the value of pressure increases with increase in positive slope and decreases with increase in negative slope.
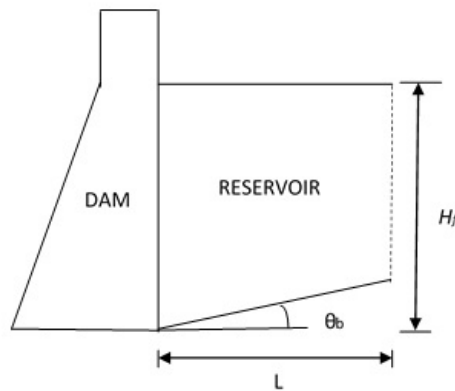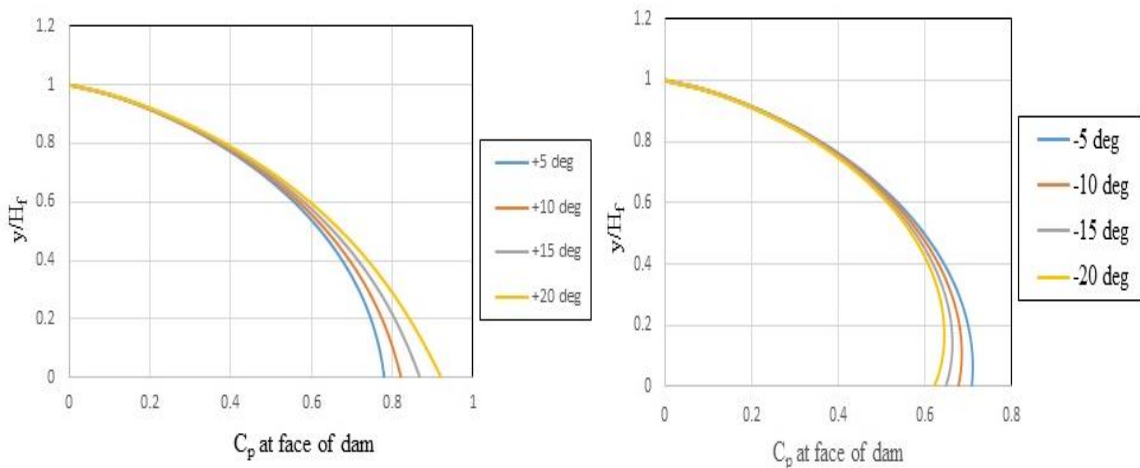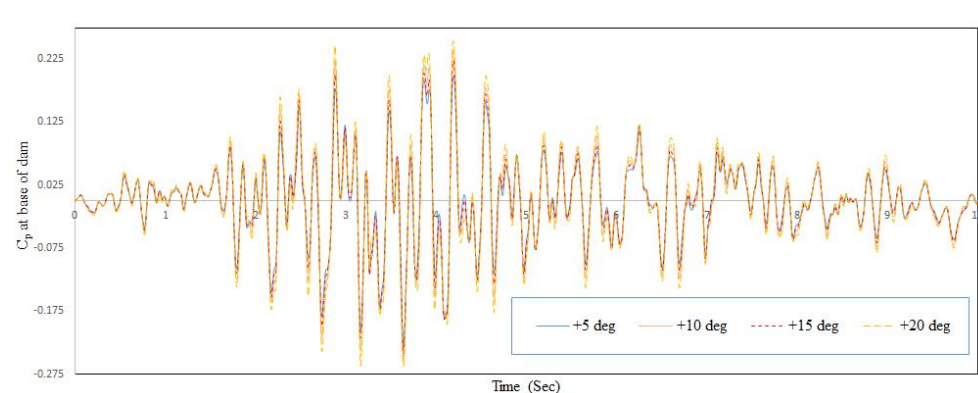

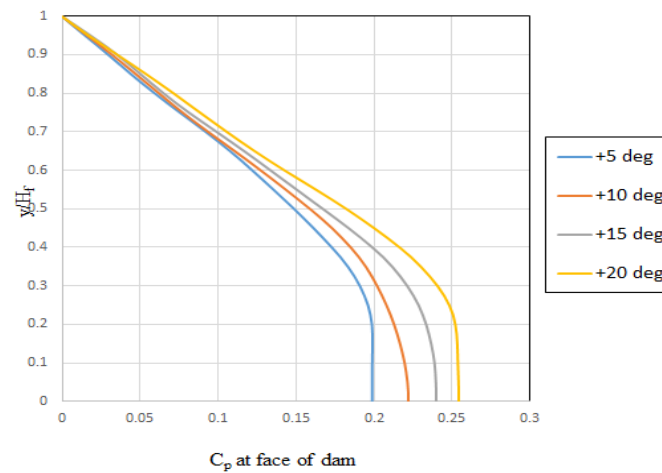Fig. 13 Geometry with inclined bottom surface of reservoir

(a) bottom slope (θ_b) positive   (b) bottom slope (θ_b) negative

Fig. 14 Distribution of pressure coefficient (C_p) at face of dam with different bottom slope (θ_b)
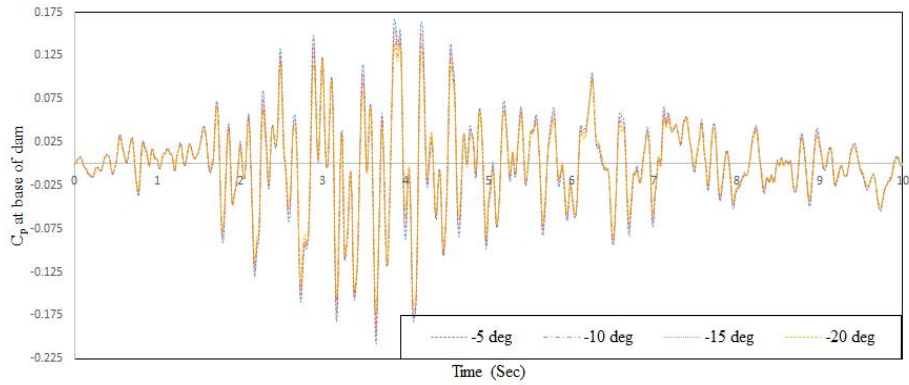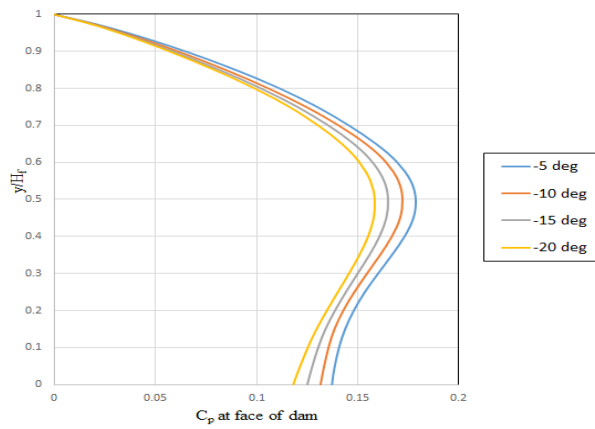
(a)

(b)

Fig. 15 (a)Time history of pressure coefficient (C_p) at base of dam with different bottom slope θ_b (positive) due to Koyna Earthquake and (b) Distribution of pressure coefficient (C_p) at face of dam with different positive bottom slope (θ_b) due to Koyna earthquake

3.2.4 Section IV

In this section distribution of pressure coefficient at face of dam studied for different values of inclined length (Li) of reservoir bottom (Fig. 17). The height of the reservoir (H_f), density of water (ρ), velocity of wave (C) in water is taken as in the Section I. Upstream face of dam is assumed as vertical with Tc/H_f =100, L/H_f = 0.5 and coefficient of bottom absorption as 0.95. Coefficient of hydrodynamic pressure distribution computed for different values of inclination of bottom slope due to harmonic loading. Figs. 18-21 present the distribution of pressure coefficient (Cp) at face of dam with different values of inclined length (Li as 0.25L,0.5L and 0.75L) for different values of positive bottom slope (θ_b =+5^0, +10^0, 15^0, +20^0). Figs. 22-25 present the distribution of pressure coefficient (C_p) at face of dam with different values of inclined length (Li as 0.25L,0.5L and 0.75L) for different values of negative bottom slope (θ_b =-5^0, -10^0, -15^0, -20^0). From these figures it is clear that the pressure at base of dam increases with increase of inclined length (Li) for positive bottom slopes and pressure decreases with increase of inclined length (Li) for negative bottom slopes.

(a)

(b)

Fig. 16 (a) Time history of pressure coefficient (C_p) at base of dam with different bottom slope θ_b (negative) due to Koyna Earthquake and (b) Distribution of pressure coefficient (C_p) at face of dam with different negative bottom slope (θ_b) due to Koyna earthquake
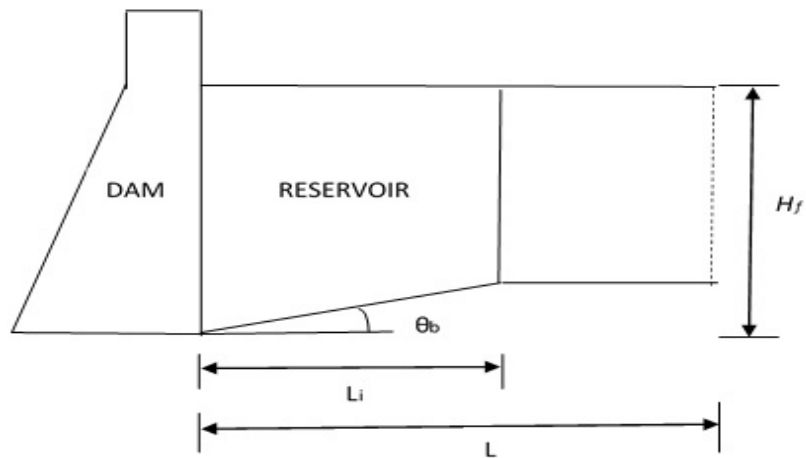

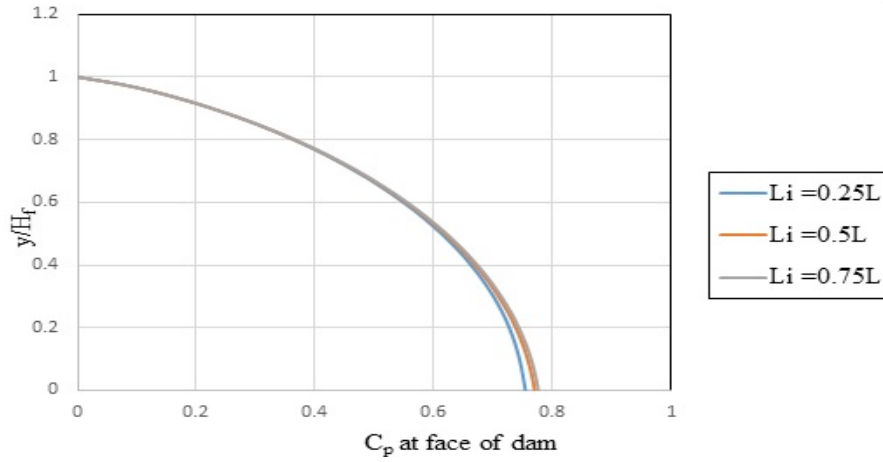Fig. 17 Geometry with inclined length of reservoir bottom

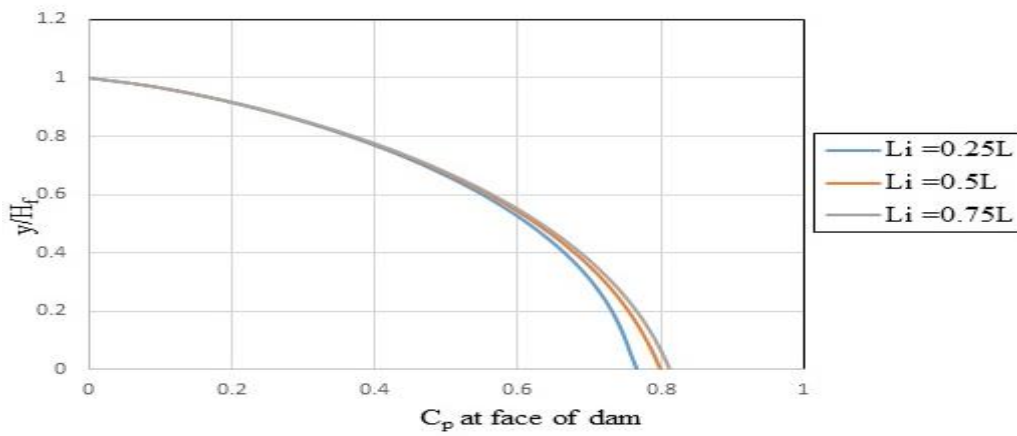Fig. 18 Distribution of pressure coefficient (C_p) at face of dam for bottom slope $\theta_b = +5^0$

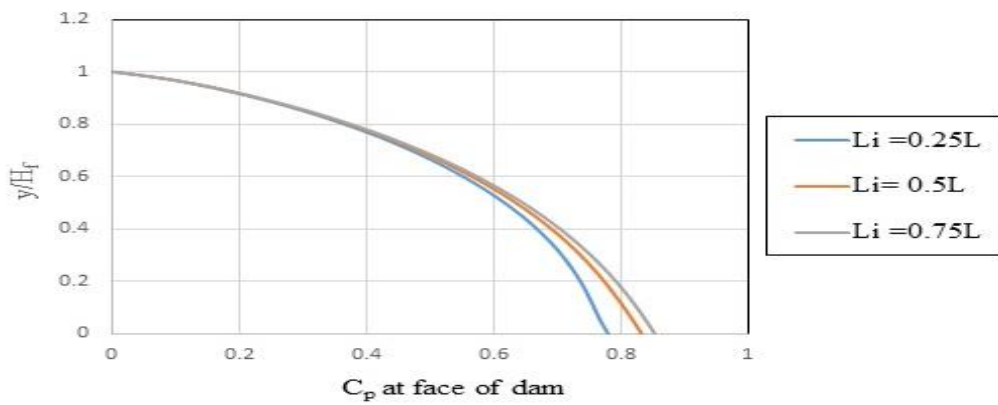Fig. 19 Distribution of pressure coefficient (C_p) at face of dam for bottom slope $\theta_b = +10^0$

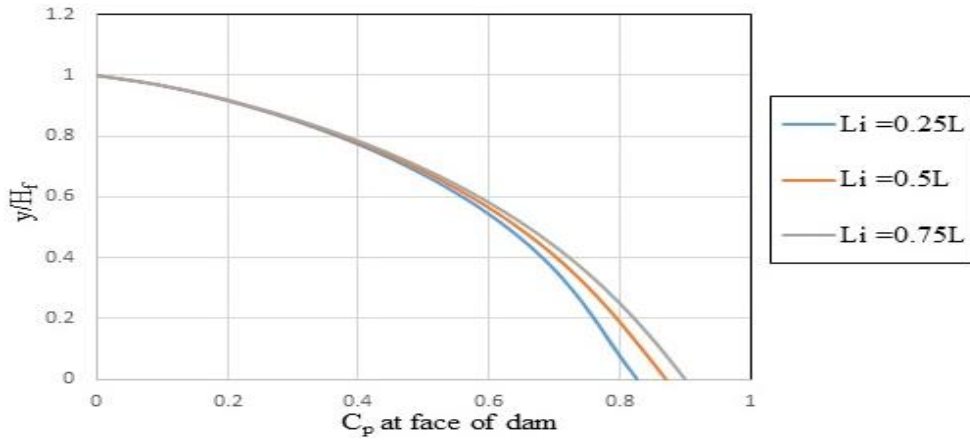Fig. 20 Distribution of pressure coefficient (C_p) at face of dam for bottom slope $\theta_b = +15^0$

Fig. 21 Distribution of pressure coefficient (C_p) at face of dam for bottom slope $\theta_b = +20^0$

Fig. 22 Distribution of pressure coefficient (C_p) at face of dam for bottom slope $\theta_b = -5^0$

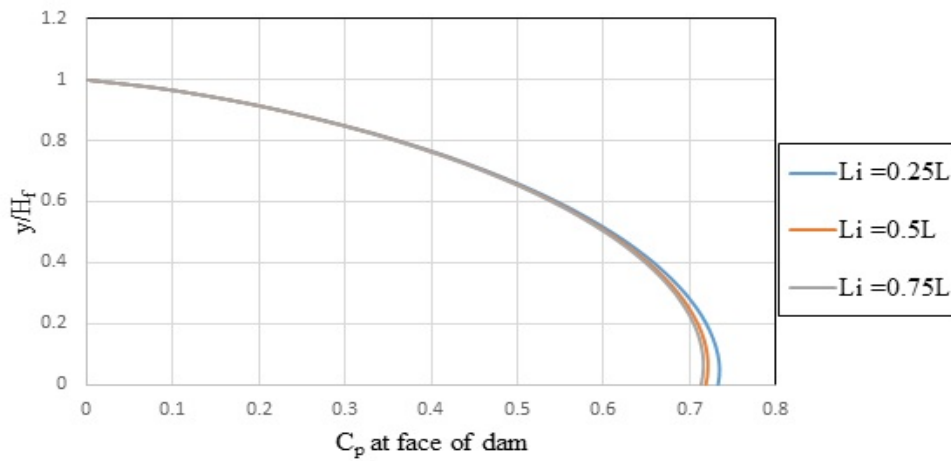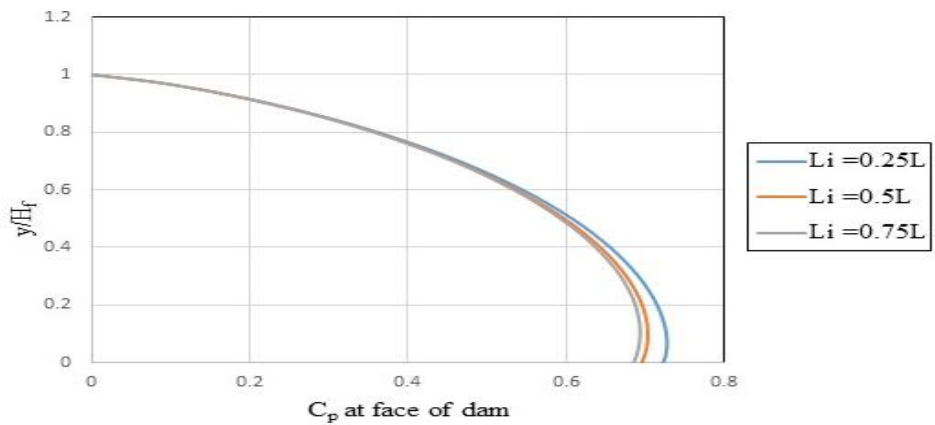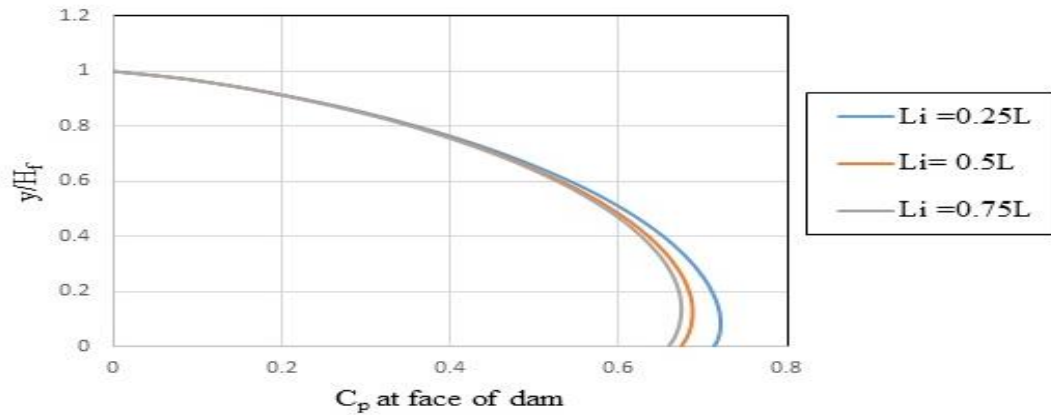Fig. 23 Distribution of pressure coefficient (C_p) at face of dam for bottom slope $\theta_b = -10^0$

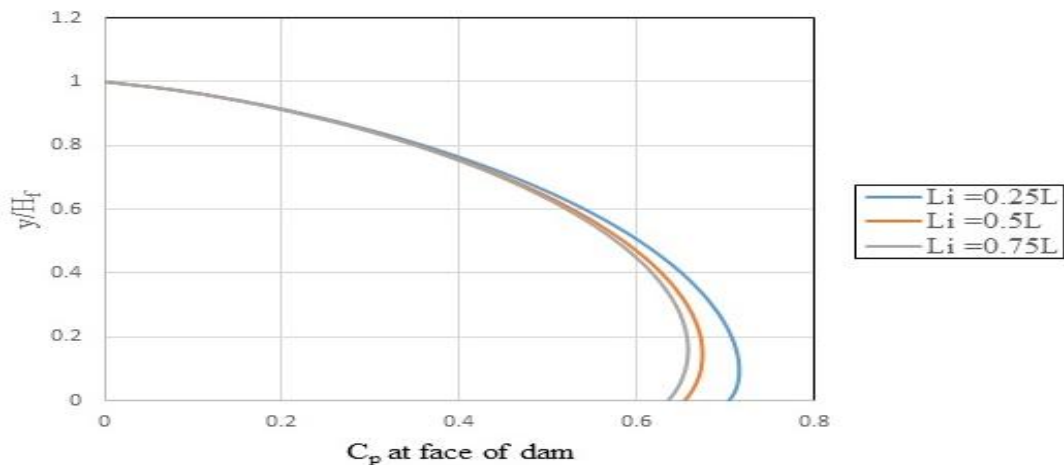Fig. 24 Distribution of pressure coefficient (C_p) at face of dam for bottom slope $\theta_b = -15^0$

Fig. 25 Distribution of pressure coefficient (C_p) at face of dam for bottom slope $\theta_b = -20^0$

4. Conclusions

Behavior of adjacent reservoir subjected to dynamic excitation is very much important for design of gravity dam. In the present work hydrodynamic pressure of infinite reservoir adjacent to gravity dam has been studied for different geometrical properties of the reservoir. From the study it is clear that the value of hydrodynamic pressure coefficient increases with the increase of inclination of dam reservoir interface. Increase in pressure is not uniform at the face of the dam due to increase of slope angle for $Tc/H_f=4$.However, increase in pressure is uniform at the face of the dam due to increase of slope angle for other frequencies. Significant differences have been noticed in velocity distribution of reservoir for different values of inclination of dam reservoir interface. There is also change in velocity profile of reservoir with change of absorption coefficient of reservoir bottom. From the study it has been also found that the value of hydrodynamic pressure at the heel of dam increases with increase of reservoir positive bottom slope angle. Hydrodynamic pressure coefficient at the

heel of dam decreases with increase of negative slope angle. Hydrodynamic pressure is also a function of inclined length of bottom of reservoir. Pressure coefficient increases at base of dam with increase of inclined length for positive slopes. However, pressure coefficient decreases at base of dam with increase of inclined length for negative slope.

References

Adhikary, R. and Mandal, K.K. (2018), "Dynamic analysis of water storage tank with rigid block at bottom", *Ocean Syst. Eng.*, **8**(1), 57-77. https:// doi.org/10.12989/ose.2018.8.1.057.

Attarnejada, R. and Bagheri, A. (2011), "Dam-reservoir interaction including the effect of vertical component of earthquake acceleration on hydrodynamic pressure", *Adv. Mater. Res.*, **255-260**, 3493-3499. https://doi.org/10.4028/www.scientific.net/AMR.255-260.3493.

Barzegar, M. and Palaniappan, D. (2020), "Numerical study on the performance of semicircular and rectangular submerged breakwaters", *Ocean Syst. Eng.*, **10**(2), 201-226. https://doi.org/10.12989/ose.2020.10.2.201.

Bouaanani, N., Paultre, P. and Proulx, J. (2003), "A closed-form formulation for earthquake-induced hydrodynamic pressure on gravity dams", *J. Sound Vib.*, **261**, 573-582.

Calayir, Y., Dumanoglu, A.A. and Bayraktar, A. (1996), "Earthquake analysis of gravity dam-reservoir systems using the eulerian and lagrangian approaches", *Comput. Struct.*, **59**(5), 877-890. https://doi.org/10.1016/0045-7949(95)00309-6.

Eftekhari, S.A. and Jafari, A.A. (2018), "A ritz procedure for transient analysis of dam–reservoir interaction", *Iran J. Sci. Technology Trans. Civil Eng.*

Gogoi, I. and Maity, D. (2006), "A non-reflecting boundary condition for the finite element modelling of infinite reservoir with layered sediment", *Adv. Water Resour.*, **29**(10), 1515-1527. https://doi.org/10.1016/j.advwatres.2005.11.004.

Hall, J.F. and Chopra, A.K. (1982), "Two-dimensional dynamic analysis of concrete gravity and embankment dams including hydrodynamic effects", *Earthq. Eng. Struct. D.*, **10**(2), 305-332. https://doi.org/10.1002/eqe.4290100211.

Humaish, A.H., Shamkhi, M.S., Al-Hachami, T.K. and Sc, B. (2018), "Seismic performance of concrete dam-reservoir system", *Int. J. Eng. Technol.*, **7**(4), 4873-4879.

Humar, J. and Roufaiel, M. (1983), "Finite element analysis of reservoir vibration", *J. Eng. Mech.*, **109**, 215-230.

Khaivi, M.P. and Sari, A. (2021), "Evaluation of hydrodynamic pressure distribution in reservoir of concrete gravity dam under vertical vibration using an analytical solution'', *Math. Problem. Eng.*, 1-9. https://doi.org/10.1155/2021/6669366.

Kucukarslan, S., Coskun, S.B. and Taskın, B. (2005), "Transient analysis of dam–reservoir interaction including the reservoir bottom effects", *J. Fluid. Struct.*, **20**(8), 1073-1084. https://doi.org/10.1016/j.jfluidstructs.2005.05.004.

Li, X., Romo, M.P.O. and Avilés, J.L. (1996), "Finite element analysis of dam-reservoir systems using an exact far-boundary condition", *Comput. Struct.*, **60**(5), 751-762. https://doi.org/10.1016/0045-7949(95)00415-7.

Maity, D. and Bhattacharyya, S.K. (1999), "Time-domain analysis of infinite reservoir by finite element method using a novel far-boundary condition", *Finite Elem. Anal. Des.*, **32**(2), 85-96. https://doi.org/10.1016/S0168-874X(98)00077-8.

Neya, B.N. and Ardeshir, M.A. (2013), "An analytical solution for hydrodynamic pressure on dams considering the viscosity and wave absorption of the reservoir", *Arab J. Sci. Eng.*, **38**, 2023-2033. https://doi.org/10.1007/s13369-013-0566-5.

Nguyen, H.X., Dinh, V.N. and Basu, B. (2021), "A comparison of smoothed particle hydrodynamics simulation with exact results from a nonlinear water wave model", *Ocean Syst. Eng.*, **11**(2), 185-201. https://doi.org/10.12989/ose.2021.11.2.185.

Pelecanos, L., Kontoe, S. and Zdravković, L. (2016), "Dam–reservoir interaction effects on the elastic dynamic response of concrete and earth dams", *Soil Dyn. Earthq. Eng.*, **82**, 138-141. https://doi.org/10.1016/j.soildyn.2015.12.003.

Saini, S.S., Bettess, P. and Zienkiewicz, O.C. (1978), "Coupled hydrodynamic response of concrete gravity dams using finite and infinite elements", *Earthq. Eng. Struct. D.*, **6**(4), 363-374. https://doi.org/10.1002/eqe.4290060404.

Samii, A. and Lotfi, V. (2007), "Comparison of coupled and decoupled modal approaches in seismic analysis of concrete gravity dams in time domain", *Finite Elem. Anal. Des.*, **431**(13), 003-1012. https://doi.org/10.1016/j.finel.2007.06.015.

Sharan, S.K. (1985), "Finite element analysis of unbounded and incompressible fluid domains", *Int. J. Numer. Method. Eng.*, **21**(9), 1659-1669. https://doi.org/10.1002/nme.1620210908.

Sharan, S.K. (1987), "Time-domain analysis of infinite fluid vibration" *Int. J. Numer. Method. Eng.*, **24**(5), 945-958. https://doi.org/10.1002/nme.1620240508.

Sharma, V., Fujisawa, K. and Murakami, A. (2019), "Space-time finite element procedure with block-iterative algorithm for dam-reservoir-soil interaction during earthquake loading", *Int. J. Numer. Method. Eng.*, **120**(3), 263-282. https://doi.org/10.1002/nme.6134.

Tsai, C.S., Lee, G.C. and Ketter, R.L. (1990), "A semi-analytical method for time-domain analyses of dam-reservoir interactions", *Int. J. Numer. Method. Eng.*, **29**(5), 913-933. https://doi.org/10.1002/nme.1620290502.

Wang, M., Chen, J., Wu, L. and Song, B. (2018), "Hydrodynamic pressure on gravity dams with different heights and the westergaard correction formula", *Int. J. Geomech.*,**18**(10). https://doi.org/10.1061/(ASCE)GM.1943-5622.0001257.

Wang, C.Z., Mitra, S. and Khoo, B.C. (2011), "Second-order wave radiation by multiple cylinders in time domain through the finite element method", *Ocean Syst. Eng.*, **1**(4), 317-336. https://doi.org/10.12989/ose.2011.1.4.317.

Wang, X., Jin, F., Prempramote, S. and Song, C. (2011), "Time-domain analysis of gravity dam–reservoir interaction using high-order doubly asymptotic open boundary", *Comput. Struct.*, **89**(7-8), 668-680. https://doi.org/10.1016/j.compstruc.2011.01.014.

Westergaard, H.M (1933), "Water pressure on dams during earthquakes", *Trans. ASCE*, **98**(2), 418-472. https://doi.org/10.1061/TACEAT.0004496.

Yichao, G., Feng, J. and Yanjie, Xu. (2019), "Transient analysis of dam–reservoir interaction using a high-order doubly asymptotic open boundary", *J. Eng. Mech.*, **145**(1), 04018119. https://doi.org/10.1061/(ASCE)EM.1943-7889.0001553.

QM